Journal of Statistical Physics, Vol. 107, Nos. 1/2, April 2002 (© 2002)

Towards a Landau–Ginzburg-Type Theory for Granular Fluids

J. Wakou,[1] R. Brito,[2] and M. H. Ernst[1]

Received February 20, 2001; accepted July 5, 2001

In this paper we show how, under certain restrictions, the hydrodynamic equations for the freely evolving granular fluid fit within the framework of the time dependent Landau–Ginzburg (LG) models for critical and unstable fluids. The granular fluid, which is usually modeled as a fluid of inelastic hard spheres (IHS), exhibits two instabilities: the spontaneous formation of vortices and of high density clusters. We suppress the clustering instability by imposing constraints on the system sizes, in order to illustrate how LG-equations can be derived for the order parameter, being the rate of deformation or shear rate tensor, which controls the formation of vortex patterns. From the shape of the energy functional we obtain the stationary patterns in the flow field. Quantitative predictions of this theory for the stationary states agree well with molecular dynamics simulations of a fluid of inelastic hard disks.

KEY WORDS: Granular fluid; instabilities; pattern formation; hydrodynamic equations; time dependent Landau–Ginzburg theory.

1. INTRODUCTION

Granular matter[(1)] consists of small or large macroscopic particles. When out of equilibrium, its dynamics is controlled by dissipative interactions, and distinguished in quasi-static flows or granular solids on the one hand, and rapid flows or granular fluids[(2)] on the other hand.

Typical realizations of granular solids are sand piles, avalanches, Saturn's rings, grain silos. Here particles remain essentially in contact, and the dynamics is controlled by gravity, friction and surface roughness.

[1] Institute for Theoretical Physics, University of Utrecht, 3508 TA Utrecht, The Netherlands; e-mail: J.Wakou@phys.uu.nl and M.H.Ernst@phys.uu.nl

[2] Departamento Física Aplicada I, Universidad Complutense, 28040 Madrid, Spain; e-mail: brito@seneca.fis.ucm.es

0022-4715/02/0400-0003/0 © 2002 Plenum Publishing Corporation

In this paper we concentrate on granular fluids. Typical examples are driven granular flows, such as Couette flow,[3] vibrated beds,[4–6] or rapid flows with some form of continuous energy input.[7] Here the dynamics is controlled by inelastic binary collisions, separated by ballistic motion of the particles. The forces are of short range and repulsive, and the system is frequently modelled as a collection of smooth inelastic hard spheres (IHS)[8] of diameter σ and mass m. Momentum is conserved during collisions, which makes the system a fluid, but energy is not conserved. In a collision, on average, a fraction ϵ of the relative kinetic energy of the colliding pair is lost, where ϵ is referred to as the degree of inelasticity. In the literature[2, 8, 9] $\epsilon = 1-\alpha^2$, usually expressed in terms of the coefficient of restitution α. Its detailed definition does not concern us here.

Here we focus on the idealized limiting case of a freely evolving rapid flow without energy input and with nearly elastic collisions, and therefore slowly cooling. This system shows[9] two interesting instabilities. When prepared in a spatially homogeneous equilibrium state, the system does not stay there, but slowly develops patterns, both in the flow field (vortices), and in the density field (clusters), the so called clustering instability.

The search for the proper macroscopic description of unstable granular fluids has been pursued by many authors.[1–10, 13–26, 29, 30] Recently, a new development, which is somewhat similar to ours, has been given by Soto *et al.*[10] These authors also study granular fluids, contained in systems that are sufficiently small, such that the clustering instability is suppressed. In these small systems the growth of vortices is very slow.

The question of interest in the present paper is: can the nonlinear hydrodynamic equations for granular fluids be fitted into the generic classification of Landau–Ginzburg-type models, as given by Hohenberg and Halperin,[11] to describe critical dynamics and hydrodynamic instabilities? The goal of this article is to illustrate how, under certain restrictions, the standard nonlinear hydrodynamic equations for the IHS fluid[2, 8] can be cast into a Landau–Ginzburg-type equation of motion for the order parameter, which can be derived from an energy functional and, more specifically, to point out which terms in the original hydrodynamic equations are responsible for the quartic terms in the Landau–Ginzburg energy functional.

The plan of the paper is as follows. In Section 2, we start with the hydrodynamic equations. The decay of the total energy at short times and the results of a linear stability analysis are briefly reviewed. In Section 3, we introduce an assumption of incompressible flows under certain restrictions on system size or time regime. Then, under these assumptions, the hydrodynamic equations are reduced to a closed equation for a scaled flow field. It is shown in Section 4 that this equation for a scaled flow field can be

cast into the form of a time-dependent Landau–Ginzburg equation for an appropriate order parameter. The shape of the energy functional is discussed and possible stationary solutions are presented. Finally, in Section 5, we make a quantitative comparison of the theoretical predictions at large times with molecular dynamics simulations of inelastic hard disks. We end with some conclusions in Section 6.

2. DYNAMIC EQUATIONS AND INSTABILITIES

We start with the hydrodynamic equations, needed to formulate the new extensions to be discussed in this paper. The macroscopic time evolution of the IHS fluid on large spatial and temporal scales can be described by the nonlinear hydrodynamic equations[12] for the local density $n(\mathbf{r}, t)$, the local flow field $\mathbf{u}(\mathbf{r}, t)$ and the local temperature $T(\mathbf{r}, t)$, supplemented with a sink term Γ accounting for the energy loss through inelastic collisions,[2, 9] i.e.,

$$\begin{aligned}
&\partial_t n + \mathbf{u}\cdot\nabla n = -n\nabla\cdot\mathbf{u},\\
&\partial_t \mathbf{u} + \mathbf{u}\cdot\nabla\mathbf{u} = -\frac{1}{mn}\nabla p + 2\nu\,\nabla\cdot\mathsf{D},\\
&\partial_t T + \mathbf{u}\cdot\nabla T = -\frac{2p}{dn}\nabla\cdot\mathbf{u} + b_T\,\nabla^2 T + 2b_\perp\,\mathsf{D}:\mathsf{D} - \Gamma
\end{aligned} \tag{1}$$

In this paper the inelasticity is always assumed to be small. For later convenience the macroscopic equations are given for a d-dimensional system. The local energy density of the IHS fluid is $e = \frac{1}{2}mnu^2 + \frac{d}{2}nT$, and p is the pressure. The shear rate $D_{\alpha\beta}$ is the symmetrized dyadic, $\{\nabla_\alpha u_\beta\}$, which is also made traceless, and $A:B = \sum_{\alpha\beta} A_{\alpha\beta}B_{\beta\alpha}$. The coefficient $b_T = 2\kappa/dn$ is proportional to the heat conductivity κ, and $b_\perp = 2m\nu/d$ to the shear viscosity ν. For simplicity of presentation the bulk viscosity has been set equal to zero, and the transport coefficients ν and κ, which depend on the local density and temperature, are taken at some fixed reference values, $\bar{n}(t)$ and $\bar{T}(t)$, to be specified later. Here Γ is the collisional cooling, and $2b_\perp\mathsf{D}:\mathsf{D}$ represents the viscous heating. The nonlinear viscous heating will be taken into account in the present paper, which is caused by gradients in the flow velocity that considerably slow down the collisional cooling process.

On the basis of kinetic theory one can derive that the rate of collisional energy loss, $\Gamma = 2\gamma_0\omega T$, is proportional to the collision frequency $\omega \sim n\sigma^{d-1}v_0$ and to the energy ϵT lost per collision,[13, 14] where $\gamma_0 = \epsilon/2d = (1-\alpha^2)/2d$. The explicit form of $\omega(T)$ is proportional to the

thermal velocity $v_0 = \sqrt{2T/m}$, and for hard sphere fluids given in refs. 15 and 16. When the system is prepared initially in a homogeneous equilibrium state, it evolves at short times as a spatially homogeneous cooling state (HCS) with a time dependent temperature, given by Haff's law[17]

$$E(t) = \frac{d}{2} T(t) = \frac{E_0}{(1+\gamma_0 \omega_0 t)^2} = E_0 \exp(-2\gamma_0 \tau) \tag{2}$$

This result is needed for later comparison. Here $E_0 = (d/2)\, T_0$ is the initial energy, and $t_0 = 1/\omega_0$ with $\omega_0 = \omega(T_0)$ is the mean free time in the initial state. The number of collisions per particle $\tau(t)$ in a time t is defined through $d\tau = \omega(T(t))\, dt$. Integration of this relation in the HCS yields $\exp(\gamma_0 \tau) = (1+\gamma_0 \omega_0 t)$.

However, this state is unstable against spatial fluctuations in density $n(\mathbf{r}, t)$, temperature $T(\mathbf{r}, t)$ and flow velocity $\mathbf{u}(\mathbf{r}, t)$. Our present theoretical understanding of these instabilities is based on a linear stability analysis[9, 14, 16, 18–21] of the hydrodynamic fluctuations in the density, $\delta n = n - \bar{n}$, temperature, $\delta T = T - \bar{T}$, and flow velocity $\mathbf{u}$. This is done by using the rescaled Fourier modes $\delta n_{\mathbf{k}}$, $\delta \tilde{T}_{\mathbf{k}} = \delta T_{\mathbf{k}}/\bar{T}$ and $\delta \tilde{\mathbf{u}}_{\mathbf{k}} \sim \mathbf{u}_{\mathbf{k}}/\sqrt{\bar{T}}$, where an overline denotes a spatial average, $\bar{a} = (1/V) \int_V d\mathbf{r}\, a(\mathbf{r})$, and $\bar{T}$ is the global temperature. Fourier transforms are defined as $f_{\mathbf{k}} = \int_V d\mathbf{r}\, e^{-i\mathbf{k}\cdot\mathbf{r}} f(\mathbf{r})$. The rescaled eigenmodes are described by $\delta a_{\mathbf{k}}(\tau) = \exp(z_\lambda(k)\, \tau)\, \delta a_{\mathbf{k}}(0)$. The well known exponential growth rates of unstable ($z_\lambda(k) > 0$) and stable ($z_\lambda(k) < 0$) modes are shown in Fig. 1 as they are needed later on to determine the system size or number of particles N, under which the present nonlinear theory is applicable.

In this paragraph we summarize the essential consequences of the linear stability analysis, and in the sequel we frequently use arguments based on them. Figure 1 shows that the transverse flow field $\mathbf{u}_{\perp\mathbf{k}}$ or shear mode ($\lambda = \perp$) with a wave number $k < k_\perp^*$ is unstable, and develops vortices. On the other hand density fluctuations couple weakly, in order $\mathcal{O}(k)$, to the heat modes ($\lambda = H$), and $z_H(k)$ in Fig. 1 shows that these fluctuations are unstable in the range $k < k_H^*$, and linearly stable in the range $k > k_H^*$, i.e., remain at thermal noise level. The stability thresholds $k_\perp^*$ and k_H^* are defined as the the root of $z_\lambda(k) = 0$ for $\lambda = \{\perp, H\}$, and are marked as black dots in the figure. The figure also shows that the growth rate $z_\perp(k)$ for the vorticity mode is much larger than the growth rate for the heat mode $z_H(k)$, which couples to the density fluctuations. This explains why vortices appear long before the density clusters start to appear. (See also refs. 9, 20, 22, 23.)

The shape of the dispersion relations for the growth rates also explains the suppression of instabilities through a reduction of the system size.[14, 19–21]

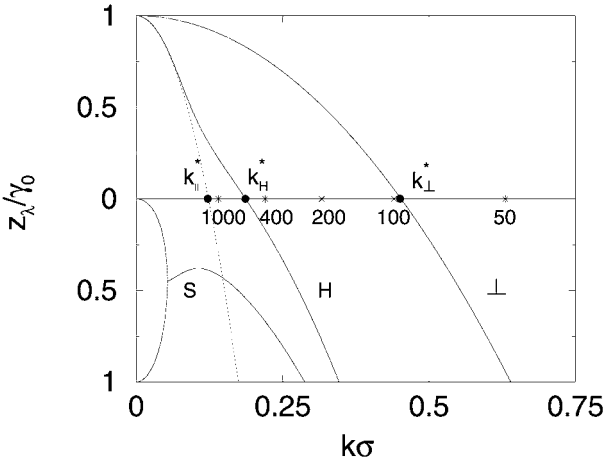

Fig. 1. Dispersion relations $z_\lambda(k)$ (from right to left) for the shear mode ($\lambda = \perp$), heat mode ($\lambda = H$) and the sound modes in the IHS fluid for an area fraction of $\phi = 0.4$ and a restitution coefficient $\alpha = 0.85$. The stars mark the location of the minimum wave vector allowed in the system, $k_0 = 2\pi/L$, for the number of particles indicated, and the black dots mark the location of the threshold values $k_a^* \sim 1/\xi_a$ with corresponding correlation lengths ξ_a where $a = (\parallel, H, \perp)$. Limiting behavior of the heat mode at $kl_0 \ll \gamma_0$, given by $z_H(k) \sim 1 - \xi_\parallel^2 k^2$ is shown as a dotted line.

Let $k_0(N) = 2\pi/L$ be the smallest wave number, allowed in a system of linear extent L at fixed density and with periodic boundary conditions. In systems with $k_H^* < k_0(N) < k_\perp^*$, there are growing vorticity modes, but all density fluctuations are stable according to a linear stability analysis. In systems with $k_0(N) < k_H^*$ the fluctuations in the density and in the flow field are unstable.[19] However, systems with $k_0(N) > k_\perp^*$ do not show any instability. The smallest allowed wave numbers $k_0(N)$ for different numbers of particles, $N = 50, 100, 200, \ldots, 1000$ at fixed packing fraction ϕ, are shown as stars in Fig. 1. The location of these stars with respect to those of the thresholds (black dots) will determine the (in)stability of the systems of size N with respect to fluctuations in density or flow field.

We finally remark that several authors have also studied nonlinear terms in the macroscopic equations for granular fluids, such as the viscous *heating* term,[9, 10, 24] and the nonlinear convective term.[25] The inclusion of the combined effects of nonlinear viscous heating and collisional cooling is essentially the mechanism driving the dynamics of dissipative granular fluids in the time regime, directly following the homogeneous cooling state.

In the present paper we will elucidate the essential physics by deriving the zeroth order contribution of the nonlinear terms in an intuitive fashion. A more systematic derivation will be published elsewhere.[26]

3. INCOMPRESSIBLE FLOWS

Instabilities and pattern formation occur in two different local fields, $\mathbf{u}$ and n, and on two different time scales, namely first patches of vorticity appear, and only much later density clusters appear.[9, 15] As explained above, the appearance of density clusters can even be further delayed, or all together suppressed by decreasing the system size.[14, 19–21] These observations suggest to analyze first the simplest nonlinear case where fluctuations in density and temperature remain small, but nonlinear viscous heating is taken into account. This would happen in the time regime following the unstable homogeneous cooling state, and possibly in the full time regime for sufficiently small systems, as suggested by a linear stability analysis. Of course the stability of solutions on the largest time scales is determined by the *full* nonlinear equations. The conditions for small n- and T-fluctuations might be realized in *incompressible* flows, where $\nabla \cdot u = 0$. Then the density remains constant in the comoving frame, and the temperature balance equation greatly simplifies. As is well known from standard fluid dynamics and from the theory of turbulence,[27, 28] flows of elastic fluids are quite *incompressible*. This implies,

$$\nabla \cdot \mathbf{u} = 0 \qquad \text{or} \qquad u_{\|\mathbf{k}} \equiv \hat{\mathbf{k}} \cdot \mathbf{u}_{\mathbf{k}} = 0 \tag{3}$$

where $u_{\|\mathbf{k}}$ is the longitudinal Fourier mode. Moreover, MD simulations and the theory of hydrodynamic fluctuations in granular flows[15, 16] show that the incompressibility assumption, $u_{\|\mathbf{k}} = 0$, remains valid down to very small wave numbers, satisfying $k\xi_{\|} \gtrsim 1$, and ultimately breaks down at the largest wavelengths, where $\xi_{\|} \sim 1/\gamma_0$ is the largest intrinsic dynamic correlation length in IHS fluid. It satisfies the inequality, $\xi_{\|} \gg \xi_{\perp} \equiv (\nu/\omega\gamma_0)^{1/2}$ for nearly elastic systems. Both correlation lengths are indicated in Fig. 1 and defined more explicitly in ref. 16.

Therefore, as a zeroth approximation to our nonlinear theory, we make the incompressibility assumption, $\nabla \cdot \mathbf{u} = 0$, following refs. 15 and 16, and the equations of motion become,

$$\begin{aligned}
&\partial_t n + \mathbf{u} \cdot \nabla n = 0, \\
&\partial_t \mathbf{u} + \mathbf{u} \cdot \nabla \mathbf{u} = -\frac{1}{mn} \nabla p + \nu \nabla^2 \mathbf{u}, \\
&\partial_t T + \mathbf{u} \cdot \nabla T = b_T \nabla^2 T + b_\perp [\nabla \mathbf{u} + (\nabla \mathbf{u})^\dagger] : \nabla \mathbf{u} - 2\gamma_0 \omega T
\end{aligned} \tag{4}$$

where $(\nabla \mathbf{u})^{\dagger}_{\alpha\beta} = \nabla_\beta u_\alpha$. This set of nonlinear equations supposedly describes the nonlinear time evolution of the temperature and flow field as long as the density fluctuations are small.

As a consequence of the incompressibility assumption the local density stays constant in time, and neither depressions, nor hot and cold regions can develop. Therefore, the pressure gradient in (4) remains negligibly small as well, so $\nabla p \simeq 0$, and the Navier–Stokes equation becomes,

$$\partial_t \mathbf{u} = -\mathbf{u} \cdot \nabla \mathbf{u} + \nu \, \nabla^2 \mathbf{u} \tag{5}$$

where the flow velocity $\mathbf{u} = \mathbf{u}_\perp$ is purely rotational with $\nabla \cdot \mathbf{u} = 0$. We also note that the divergence of Eq. (5), in combination with $\nabla \cdot \mathbf{u} = 0$, reduces to $(\nabla \mathbf{u}) : (\nabla \mathbf{u}) = 0$ at all times.

Next we consider the temperature balance equation, which involves two processes: the diffusion process of heat conduction, where Fourier modes $T_{\mathbf{k}}$ decay with a rate $b_T k^2$, and the global process of collisional cooling and nonlinear viscous heating, describing the decay of $T_{\mathbf{k}}$ for $k \to 0$, or equivalently of $\bar{T}(t) \equiv (1/V) \int_V d\mathbf{r} \, T(\mathbf{r}, t)$, referred to as global temperature.

To split off the behavior of $\bar{T}(t)$ from Eq. (4) we take the spatial average of the T-equation, so that the nonlinear terms $\mathbf{u} \cdot \nabla T$ and $\nabla \mathbf{u} : \nabla \mathbf{u}$ vanish because of incompressibility assumption, yielding for the nonlinear evolution of the global temperature:

$$\partial_t \bar{T} = b_\perp \, \overline{|\nabla \mathbf{u}|^2} - 2\gamma_0 \omega \bar{T} \tag{6}$$

where overlines denote spatial averages. We have introduced the notation $|\mathsf{A}|^2 = \sum_{\alpha\beta} |A_{\alpha\beta}|^2$, for a second rank tensor A. The transport coefficient $b_\perp$ and collision frequency ω are functions of the spatially average density $\bar{n} = N/V$ and temperature $\bar{T}(t)$ (see "reference values" below Eq. (1)). This is allowed as long as the local fluctuations $\delta n = n - \bar{n}$ and $\delta T = T - \bar{T}$ remain small.

The new evolution Eqs. (5) and (6) contain the time dependent coefficients $b_\perp$, ω and ν, which are proportional to $\bar{v}_0(t) \equiv (2\bar{T}(t)/m)^{1/2}$. Therefore, it is convenient to introduce the scaled field $\tilde{\mathbf{u}} = \mathbf{u}/\bar{v}_0$, and the scaled time τ, defined as $d\tau = \omega(\bar{T}) \, dt$. The final macroscopic evolution equations then become,

$$\begin{aligned}
\partial_\tau \ln \bar{T} &= \frac{4}{d} \mathscr{D}_\perp \, \overline{|\nabla \tilde{\mathbf{u}}|^2} - 2\gamma_0, \\
\partial_\tau \tilde{\mathbf{u}} + l_0 \, \tilde{\mathbf{u}} \cdot \nabla \tilde{\mathbf{u}} &= \mathscr{D}_\perp \, \nabla^2 \tilde{\mathbf{u}} - \frac{1}{2} (\partial_\tau \ln \bar{T}) \, \tilde{\mathbf{u}} \\
&= \gamma_0 \tilde{\mathbf{u}} + \mathscr{D}_\perp \, \nabla^2 \tilde{\mathbf{u}} - \frac{2}{d} \mathscr{D}_\perp \, \overline{|\nabla \tilde{\mathbf{u}}|^2} \, \tilde{\mathbf{u}}
\end{aligned} \tag{7}$$

where $l_0 = \bar{v}_0/\omega$ is the (time-independent) mean free path. The last equation is a closed equation for $\tilde{\mathbf{u}}$, and the physically consistent solutions need to obey the relation $\nabla \cdot \mathbf{u} = 0$. The global temperature is slaved by the flow field. The rescaled vorticity diffusion coefficient, defined as $\mathscr{D}_\perp = \nu/\omega$, is independent of time. The first term on the right hand side of the equation for $\tilde{\mathbf{u}}$ accounts for the instability, the second for the vorticity diffusion and the last one for the saturation effects, caused by the nonlinear viscous heating. It slows down the growth of unstable $\mathbf{k}$-modes, and may ultimately lead to a steady state for $\tilde{\mathbf{u}}$. For large times nonlinear effects will induce density inhomogeneities, even in small systems with $k_H^* < k_0(N) < k_\perp^*$. If these density inhomogeneities do not remain small enough, the above equations (5) and (6) are no longer valid.

4. SPONTANEOUS SYMMETRY BREAKING

In this section we will drop the nonlinear convective term $\tilde{\mathbf{u}} \cdot \nabla \tilde{\mathbf{u}}$, but at the end of our analysis we admit out of all possible solutions only those that satisfy Eq. (7) with the convective term included.

The final equation for the rescaled $\mathbf{u}$-field has the form of the Landau–Ginzburg equation of motion for a *non-conserved* order parameter. This can be made more explicit by introducing the order parameter $\mathsf{S} = \nabla \tilde{\mathbf{u}}$, and applying ∇ to the $\mathbf{u}$-equation in (7) with the result,

$$\begin{aligned} \partial_\tau \mathsf{S} &= (\gamma_0 + \mathscr{D}_\perp \nabla^2)\, \mathsf{S} - \frac{2}{d}\, \mathscr{D}_\perp\, \overline{|\mathsf{S}|^2}\, \mathsf{S} \\ &= -V\, \delta \mathscr{H}[\mathsf{S}]/\delta \mathsf{S}^\dagger \end{aligned} \tag{8}$$

where the last line contains the functional derivative of the energy functional $\mathscr{H}[\mathsf{S}]$, defined as

$$\mathscr{H}[\mathsf{S}] = -\frac{1}{2}\gamma_0\, \overline{|\mathsf{S}|^2} + \frac{1}{2}\mathscr{D}_\perp\, \overline{|\nabla \mathsf{S}|^2} + \frac{1}{2d}\mathscr{D}_\perp (\overline{|\mathsf{S}|^2})^2 \tag{9}$$

In our further considerations it is more convenient to use Fourier modes. Moreover $\mathbf{u}_\mathbf{k} = \mathbf{u}_{\perp\mathbf{k}}$, because of the assumption of incompressibility, and $\mathsf{S}_\mathbf{k} \equiv \mathbf{k}\tilde{\mathbf{u}}_{\perp\mathbf{k}}$. Then we obtain the equation of motion,

$$\begin{aligned} \partial_\tau \mathsf{S}_\mathbf{k} &= -V^2\, \delta \mathscr{H}[\mathsf{S}]/\delta \mathsf{S}_\mathbf{k}^\dagger \\ &= \left\{ \gamma_0 - \mathscr{D}_\perp k^2 - \frac{2\mathscr{D}_\perp}{dV^2} \sum_\mathbf{q} |\mathsf{S}_\mathbf{q}|^2 \right\} \mathsf{S}_\mathbf{k} \end{aligned} \tag{10}$$

with an energy functional,

$$\mathscr{H}[\mathsf{S}] = \frac{1}{2V^2}\sum_{\mathbf{k}} (-\gamma_0 + \mathscr{D}_\perp k^2)\,|\mathsf{S}_\mathbf{k}|^2 + \frac{\mathscr{D}_\perp}{2d}\left(\frac{1}{V^2}\sum_{\mathbf{k}} |\mathsf{S}_\mathbf{k}|^2\right)^2 \tag{11}$$

where the wave number $\mathbf{k} = \mathbf{0}$ does not contribute.

The energy in (9) and (11) resembles a Landau free energy form for a *tensorial order parameter* $\mathsf{S} = \nabla\tilde{\mathbf{u}}$ with $\mathrm{tr}\,\mathsf{S} = \nabla\cdot\tilde{\mathbf{u}} = 0$, which is in fact the shear rate or rate of deformation tensor. It has a quartic term S^4, and a quadratic term S^2 with a coefficient that vanishes at a critical threshold $k_\perp^* = (\gamma_0/\mathscr{D}_\perp)^{1/2}$. It differs from the standard Landau free energy in that the quartic term contains summations over two totally independent wave numbers.

These results are very interesting. If the energy functional has a minimum, then there is a fixed point solution, $\mathsf{S}_\mathbf{k}(\infty)$, that is approached for large times. They are found by setting the right hand side of (10) equal to zero, i.e.,

$$\left\{\gamma_0 - \mathscr{D}_\perp k^2 - \frac{2\mathscr{D}_\perp}{dV^2}\sum_{\mathbf{q}} |\mathsf{S}_\mathbf{q}|^2\right\}\mathsf{S}_\mathbf{k} = 0 \tag{12}$$

We will show that depending on the parameter, $k_0 = 2\pi/L$, being above or below the threshold value $k_\perp^* \equiv \sqrt{\gamma_0/\mathscr{D}_\perp}$, the fixed point value of the order parameter, $\{\mathsf{S}_\mathbf{k}(\infty)\}$, is *vanishing* or *non-vanishing*. A stable fixed point with some non-vanishing Fourier components indicates that the system approaches a non-equilibrium steady state with a stationary pattern in the flow field, and spontaneous symmetry breaking has occurred.

Consider the right hand side of (10), and observe that the expression between curly brackets is necessarily *negative* for $k > k_\perp^*$, and the Fourier mode $\mathsf{S}_\mathbf{k}$ decays to zero. If the smallest possible wave number satisfies, $k_0 > k_\perp^*$, *all* $\mathsf{S}_\mathbf{k}$ decay to zero, and there is no spontaneous symmetry breaking. The system remains spatially homogeneous. However, if $k_0 < k_\perp^*$, then the right hand side of (10) may become zero and even positive. There is the possibility of stationary and of exponentially growing solutions, and the expression inside brackets in Eq. (10) may vanish for a non-vanishing value of $\mathsf{S}_\mathbf{k}(\infty)$, i.e., there is an extremum determined by the condition,

$$\frac{1}{V^2}\sum_{\mathbf{q}} |\mathsf{S}_\mathbf{q}|^2 = \frac{d}{2}(\gamma_0 - \mathscr{D}_\perp k^2)/\mathscr{D}_\perp \tag{13}$$

If the extremum is a saddle point then there are directions of exponentially growing solutions. The fixed point $\{\mathsf{S}_\mathbf{k}(\infty) = 0$ for any $\mathbf{k}\}$ is a saddle

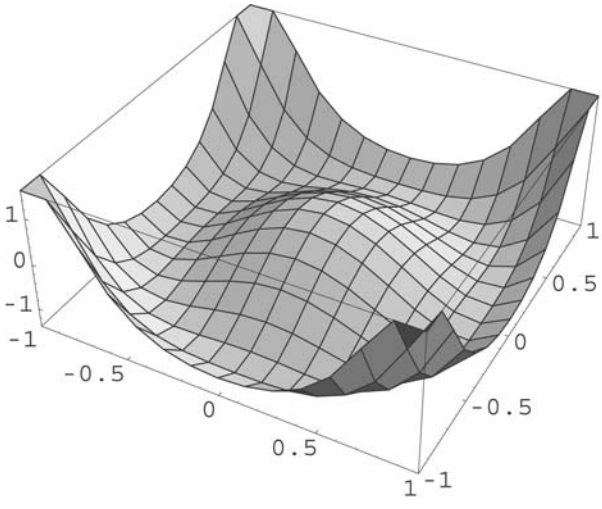

Fig. 2. Landscape plot of the energy $\mathscr{H}[\mathsf{S}]$ in the $\mathsf{S}_{\mathbf{k}_0}$-subspace.

point. One can also show (See Appendix A) that all fixed point solutions with non-vanishing $\mathsf{S}_{\mathbf{k}}$ for any $|\mathbf{k}| \neq k_0$ are saddle points, and that the only non-vanishing solution $\{\sum_{\mathbf{k}_0} |\mathsf{S}_{\mathbf{k}_0}|^2 \neq 0, \mathsf{S}_{\mathbf{k}} = 0 \text{ if } |\mathbf{k}| \neq k_0\}$, where $\sum_{\mathbf{k}_0}$ is summation over $\mathbf{k}_0$ with $|\mathbf{k}_0| = k_0$, is a stable fixed point with an infinitely degenerate minimum, given symbolically by the Mexican hat shape as illustrated in Fig. 3. The condition (13) for $\mathbf{u}_{\perp\mathbf{k}}$ with $|\mathbf{k}| = k_0 = 2\pi/L$ in d-dimensions is then

$$\frac{1}{V^2} \sum_{\alpha=1}^{d} |\tilde{\mathbf{u}}_{\mathbf{k}_{0\alpha}}|^2 = \frac{d}{4} (\gamma_0 - \mathscr{D}_\perp k_0^2)/\mathscr{D}_\perp k_0^2 \tag{14}$$

where $\mathbf{k}_{0\alpha} = k_0 \hat{\mathbf{e}}_\alpha$ and $\hat{\mathbf{e}}_\alpha$ is a unit vector in the direction α ($\alpha = \{1, 2, \ldots, d\}$). As the solutions of these equations have to satisfy Eq. (3), the Fourier components can be written as

$$\tilde{\mathbf{u}}_{\mathbf{k}_{0\alpha}} = \frac{1}{2} V \sum_{\beta(\neq\alpha)} \hat{\mathbf{e}}_\beta A_{\alpha\beta}\, e^{i\theta_{\alpha\beta}} \tag{15}$$

where the phases $\theta_{\alpha\beta}$ and amplitudes $A_{\alpha\beta}$ are $2d(d-1)$ real numbers. On account of (14) the amplitudes satisfy the relations

$$A_0^2 \equiv \sum_{1 \leqslant \alpha \neq \beta \leqslant d} \sum A_{\alpha\beta}^2 = d(\gamma_0 - \mathscr{D}_\perp k_0^2)/\mathscr{D}_\perp k_0^2 \tag{16}$$

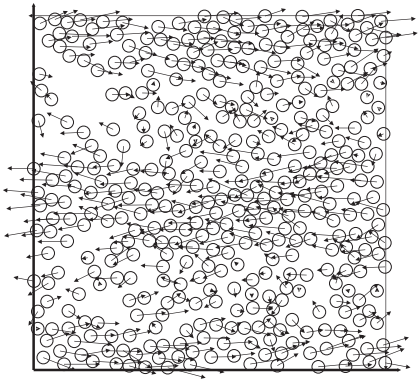

$\phi = 0.4$
$k_0 = 0.224$
$\alpha = 0.85$
$\omega_0 = 4.14$
$\mathscr{D}_\perp = 0.334$
$\bar{T}(600) = 2.37 \times 10^{-10}$
$E(600) = 1.27 \times 10^{-9}$
$\bar{v}_0(600) = 2.18 \times 10^{-5}$

Fig. 3. Left: Instantaneous configuration of the IHS fluid after $\tau = 600$ collisions per particle for a system of $N = 400$ discs at area fraction of $\phi = 0.4$, which clearly exhibits the velocity profile as well as the high density state. The arrows indicate the instant velocity of the particles and the circles the actual size. A shear flow is observed in agreement with the solution of the nonlinear equations given in Eq. (18). Right: Numerical data for this and subsequent plots. Last three entries are at $\tau = 600$. Units are chosen such that initial temperature $T_0 = 1$, mass $m = 1$, and sphere diameter $\sigma = 1$.

The stable stationary solutions in real space are then

$$\tilde{\mathbf{u}}_0(\mathbf{r}) = \sum_{\alpha \neq \beta} \sum A_{\alpha\beta}\, \hat{\mathbf{e}}_\beta \cos(k_0 r_\alpha + \theta_{\alpha\beta}) \tag{17}$$

Out of this set of solutions we select those that satisfy the full nonlinear Eq. (7) with the convective term included, i.e., we determine the $d(d-1)$ amplitudes $A_{\alpha\beta}$ such that the relation, $\tilde{\mathbf{u}}_0 \cdot \nabla \tilde{\mathbf{u}}_0 = \mathbf{0}$, is satisfied. This yields d conditions. For the two-dimensional case only *two* fixed point solutions remain, instead of infinitely many degenerate minima, i.e.,

$$\begin{aligned} \tilde{\mathbf{u}}_0(x) &= \hat{\mathbf{e}}_y A_0 \cos(k_0 x + \theta_x) \\ \tilde{\mathbf{u}}_0(y) &= \hat{\mathbf{e}}_x A_0 \cos(k_0 y + \theta_y) \end{aligned} \tag{18}$$

The symmetry of the steady state is spontaneously broken, and spontaneous fluctuations in the initial state determine which of these two minima will be reached.

In summary, the equation, describing the growth dynamics of vortices in granular fluids, *without* the convective term is described by a time dependent Landau–Ginzburg equation for a non-conserved order parameter, $\mathbf{S} = \nabla \tilde{\mathbf{u}}$, derived from an energy functional with a *continuous* set of degenerate minima, having the shape of a Mexican hat. The last observation may suggest that unstable granular fluids have some resemblance to

Model H[11] which has a similar energy surface in the neighborhood of its stable fixed points. However, this is not the case. Addition of the nonlinear convective term to Eq. (8) selects out of this infinite set of minima only subsets of admissible solutions. In two dimensions only *two* distinct minima survive. Therefore, the unstable two-dimensional IHS fluid has a greater resemblance to spinodal decomposition for a non-conserved order parameter, which belongs to the universality class of Model A.[11] It should be noted that the complete solution of Eq. (7) with the convective term included may have a larger set of physically acceptable solutions. However, we have not been able to find any.

5. MD-SIMULATIONS

In this section we present results obtained from our theory and compare the theoretical predictions with the results of computer simulations of small systems in two dimensions.

A snapshot of a typical configuration for a small system with $k_H^* < k_0 < k_\perp^*$ at large times $\tau \gg \tau_{cr} = L^2/\mathscr{D}_\perp$ is shown in Fig. 3. Here τ_{cr} is a characteristic time when a typical size of vortices becomes comparable to the system size L. A shear flow with variation of the u_x-component in the y-direction is observed. Individual v_x-components of the particle velocities are plotted in Fig. 4 versus their y-coordinate. A fit to a sinusoidal curve (solid line) shows that the solution described in (18) is realized. It should also be noted that the presence of a velocity field makes the local energy per particle different from the local temperature. These two quantities are clearly different in Fig. 5.

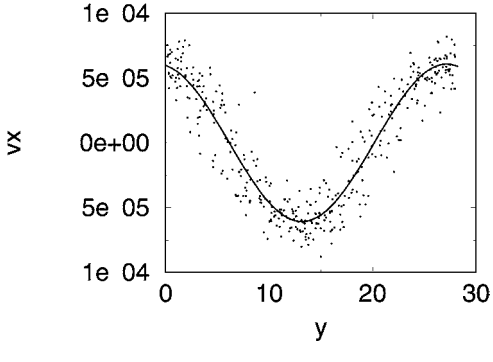

Fig. 4. Profile of shear flow in Fig. 3. Dots represent the instantaneous velocities of the particles; the solid line is a fit to the sinusoidal function, described in Eq. (18), with amplitude $A_{\text{sim}}/\bar{v}_0 \simeq 2.78$ and theoretical prediction $A_0 \simeq 2.51$.

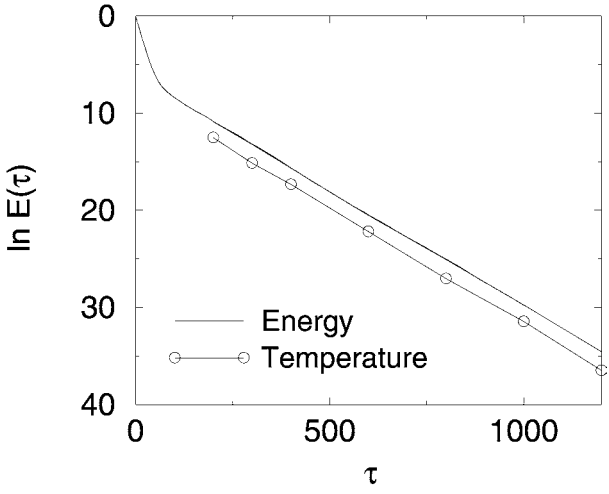

Fig. 5. Behavior of the temperature (circles) as a function of the number of collisions per particle τ. It is compared with the energy per particle (solid line), demonstrating the validity of Eq. (24). For instance, at $\tau = 600$ one finds by simulation $(E/\bar{T})_{\text{sim}} \simeq 5.38$ with a theoretical value $\gamma_0/\mathscr{D}_\perp k_0^2 \simeq 4.14$. In the stationary state there is a clear distinction between total energy per particle E, and the energy T in the comoving frame.

We assume that the number of collisions τ in the simulations of Figs. 3 and 4 is sufficiently large, so that the components $\tilde{\mathbf{u}}_{\mathbf{k}}$ are very close to their fixed point values. Then, the relation, $\mathscr{D}_\perp \overline{|\nabla \tilde{\mathbf{u}}|^2} = \frac{1}{2} d(\gamma_0 - \mathscr{D}_\perp k_0^2)$, follows from (17), and $\partial_\tau \ln \bar{T} \simeq -2\mathscr{D}_\perp k_0^2$ from (7). The global temperature for large times, i.e., $\tau \gg \tau_{cr}$, becomes,

$$\bar{T} \simeq T_e \exp(-2\mathscr{D}_\perp k_0^2 \tau) \tag{19}$$

Equation (19) gives the temperature as a function of τ. The integration constant *cannot* be determined from the theory, but a fit of (19) to the simulation data in Fig. 5 for $\tau > 200$ yields $T_e \simeq 3.87 \times 10^{-4}$. We also note that the mode coupling theory of ref. 23, developed for thermodynamically large systems, gives the same decay rate for the total energy, when this theory is applied to the *small* systems, considered here. For these small systems the Fourier sum $(1/V)\sum_{\mathbf{q}}$ can not be replaced by $\int d\mathbf{q}/(2\pi)^d$, but is essentially given by its first term only.

The relation between τ and t is defined through $d\tau = \omega(\bar{T})\, dt$, where the collision frequency ω is proportional to the square root of $\bar{T}$, i.e.,

$$\frac{d\tau}{dt} = \omega(\bar{T}) = \omega_0 \sqrt{\frac{\bar{T}}{T_0}} \simeq \omega_0 \sqrt{\frac{T_e}{T_0}} \exp\left[-\mathscr{D}_\perp k_0^2 \tau\right] \tag{20}$$

where $\omega_0 = \omega(T_0)$ is the collision frequency at the initial time. As ω can be measured directly as a function of t in MD simulations, it yields an independent determination of T_e with the result $T_e \simeq 3.68 \times 10^{-4}$. Integration of (20) yields,

$$\exp(\mathscr{D}_\perp k_0^2 \tau) \simeq \omega_0 \sqrt{\frac{T_e}{T_0}}\, \mathscr{D}_\perp k_0^2 (t - t_e) \tag{21}$$

valid for $(t - t_e)$ large. After eliminating τ from Eq. (19) and (21) we obtain the global temperature for asymptotically large time t as,

$$\bar{T} \simeq \frac{T_0}{(\omega_0 \mathscr{D}_\perp k_0^2)^2} \frac{1}{(t - t_e)^2} \tag{22}$$

where visual inspection of Fig. 6 shows that $t_e \simeq 10^4$. The temperature shows *algebraic decay* with the same exponent as in Haff's law (2), but the prefactor in Haff's law does neither depend on the system size, nor on the dimensionality. In (22) it is proportional to $L^4 \sim N^{4/d}$, whereas the prefactor in Haff's law is independent of the system size (see Fig. 6).

Once we have $\bar{T}$, we can calculate the averaged energy per particle, as,

$$E = \frac{1}{n}\left[\overline{\frac{m}{2} n\, \mathbf{u}^2 + \frac{d}{2} nT}\right] = \bar{T}\left[\overline{\tilde{\mathbf{u}}^2} + \frac{d}{2}\right] \tag{23}$$

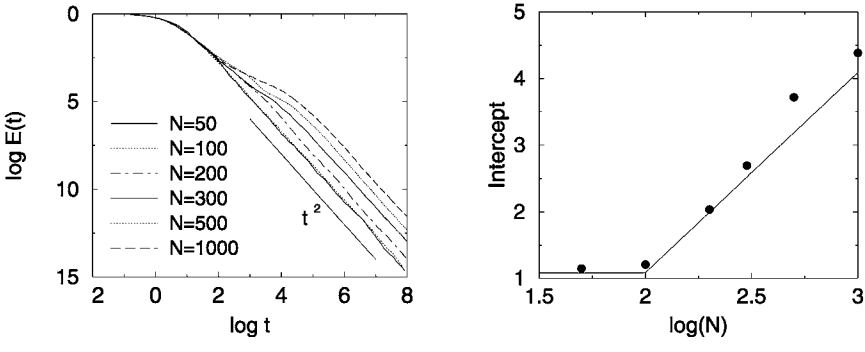

Fig. 6. Left: Simulation results of the behavior of $E(t)$ as a function of t for N particles. At large times ($t \gtrsim 10^4$ for $\phi = 0.4$ and $\alpha = 0.85$), a power law tail $\sim 1/t^2$ is observed. The coefficient B, defined in (25), is on average 2.3×10^{-5} with a theoretical value $B \simeq 1.2 \times 10^{-5}$. Right: the amplitude of the tail is proportional to N^3. Here the solid line is the result of the theory, Eq. (25), while the dots are simulation results extracted from the left panel.

where local density variations are supposedly small and the relation $\mathbf{u} = \bar{v}_0 \tilde{\mathbf{u}}$ has been used. Combination of this result with (17) yields,

$$E \simeq \frac{d\gamma_0}{2\mathscr{D}_\perp k_0^2} \bar{T} \tag{24}$$

This shows that at long times, the energy and temperature are proportional, and differ by a non-trivial factor. Therefore, energy decays exponentially when expressed in terms of τ (see (19)), with the same decay rate as the global temperature. This property is observed by MD simulations, as shown in Fig. 5. From (22) and (24) the decay of the energy per particle in terms of t in the long time limit is given by

$$E(t) \simeq \frac{d\gamma_0 \, T_0}{2\omega_0^2 (\mathscr{D}_\perp k_0^2)^3} \frac{1}{(t-t_e)^2} \equiv B \frac{N^{6/d}}{(t-t_e)^2} \tag{25}$$

Hence, if we vary the number of particles N, at fixed packing fraction ϕ, the amplitude of t^{-2}-decay of the energy is proportional to N^3 in two-dimensional systems, or to $N^{6/d}$ in d-dimensional systems. Comparison of Eq. (25) with simulations is shown in Fig. 6. It would also be interesting to compare the coefficient B in (25) with the simulation results of ref. 29 for the IHS fluid which have been performed in five and six dimensions.

Finally, by extending the present analysis one can also calculate the local density and local temperature with the result,[26]

$$\begin{aligned} \delta\tilde{T} &\equiv \frac{T(y)}{\bar{T}} - 1 \simeq -\frac{\nu A_0^2}{4b_T} \cos[2(k_0 y + \theta_y)] \\ \delta\tilde{n} &\equiv \frac{n(y)}{\bar{n}} - 1 \simeq \frac{\nu A_0^2 \, \bar{T} \left(\dfrac{\partial p}{\partial T} \right)}{4 b_T \, \bar{n} \left(\dfrac{\partial p}{\partial n} \right)} \cos[2(k_0 y + \theta_y)] \end{aligned} \tag{26}$$

where $\bar{n} = N/V$, and θ_y is the same phase factor as given in (18). The derivation will be published elsewhere.[26] It means that the density and temperature inhomogeneities show a period which is half the period of the shear flow profile. The relation between the spatial periods has already been observed in ref. 9 in MD simulations of a fluid of two-dimensional hard disks, and in ref. 24 in Direct Monte Carlo simulations of the Boltzmann equation for an IHS gas, without analytical predictions for the amplitudes. In ref. 10, an analytical result that is similar to (26) is given for systems which are close to the stability thresholds $k_\perp^*$. Figure 7 shows the

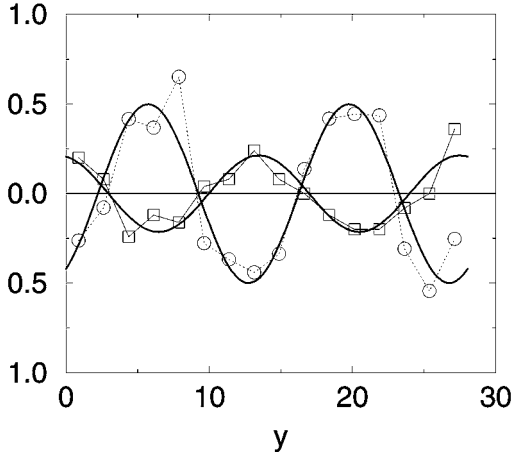

Fig. 7. Density (squares) and temperature (circles) inhomogeneities, $\delta\tilde{n}$ and $\delta\tilde{T}$ at $\tau = 600$. The solid lines correspond to nonlinear fits to sinusoidal functions of half the period in (26) with amplitudes $A_{T(\mathrm{sim})} = 0.5$ and $A_{n(\mathrm{sim})} = 0.24$, and theoretical predictions given by (26) are $\nu A_0^2/4b_T = 0.32$ and $\nu A_0^2 \bar{T}(\partial p/\partial T)/4b_T\, \bar{n}(\partial p/\partial n) = 0.14$, respectively. The simulated ratio of $\delta\tilde{T}$- to $\delta\tilde{n}$ amplitudes is here 2.0, and the theoretical prediction is 2.3.

observed density and temperature inhomogeneities. A fit to a sinusoidal curve supports the temperature and density profiles given by (26).

As shown in Eq. (26), the temperature and density inhomogeneities are in opposite phase, implying that dense regions are cold, and the dilute regions hot. The amplitudes are such that the overall pressure is constant, as we have assumed in the course of the paper.

6. CONCLUSIONS

Under the restrictions imposed in our derivations, as discussed in Section 3, we have shown that the unstable dynamics and formation of vortex patterns in the flow field of a freely evolving fluid of inelastic hard spheres (IHS) can be cast in the form of a time-dependent Landau–Ginzburg-type model for a non-conserved order parameter. In the two-dimensional case (but not for $d \geqslant 3$) the growth of the vortex pattern in the IHS fluid is qualitatively similar to spinodal decomposition for a non-conserved scalar order parameter, referred to as model A in the Hohenberg–Halperin classification.[11] A formal analogy between the unstable IHS fluid in two-dimensions and spinodal decomposition, based on the dispersion relations of the unstable Fourier modes (see Fig. 1), has been pointed out before in ref. 22. A difference between our model and model A is that the energy functional (9) contains a quartic term with summations over two independent wave numbers. This implies a non-local interaction of the

order parameter $\mathbf{S} = \nabla\tilde{\mathbf{u}}$. The non-local interaction is caused by the scaled field $\tilde{\mathbf{u}} = \mathbf{u}/\bar{v}_0 \sim \mathbf{u}/\sqrt{\bar{T}}$. Because the global temperature $\bar{T}$ is determined by $\mathbf{S}$ in all space (see Eq. (6)), the evolution of a local order parameter $\mathbf{S}$ is affected by $\mathbf{S}$ at any other points in space through $\bar{T}$.

We have shown that nonlinear viscous heating gives rise to a quartic term in the energy functional, which is responsible for saturation of unstable vorticity modes. Unstable vorticity modes initially grow as predicted by the linear stability analysis, but eventually saturate because of nonlinear viscous heating. The influence of nonlinear viscous heating on the formation of temperature inhomogeneities and clustering has been pointed out and studied by Goldhirsch and Zanetti,[9] and investigated in more detail by Brey *et al.*,[24] by comparing the results of a hydrodynamic model with viscous heating, using direct Monte Carlo simulation of the Boltzmann equation.

The theoretical predictions of our theory for the flow field and the decay of the energy are in quantitative agreement with MD simulations of small systems as shown in Section 5. They support the intuitive arguments used in deriving the evolution equation (7) for the scaled flow field $\tilde{\mathbf{u}}$, presented in Section 3. Moreover, the results presented here can be obtained as the lowest order approximation in a systematic expansion.[26] Density and temperature *inhomogeneities* are only found in the next order of approximation.

It is worth mentioning that results of the present theory and the first order corrections are consistent with the results of a nonlinear analysis by Soto *et al.*[10] of systems which are close to the stability thresholds $k_\perp^*$. If the smallest wave number of the system k_0 is slightly smaller than $k_\perp^*$, vorticity modes with the wave number k_0 grow so slowly that the remaining hydrodynamic modes are enslaved by these vorticity modes. On the basis of an adiabatic elimination method, they obtained amplitude equations for the vorticity modes with k_0, and the stationary inhomogeneous density and temperature with a period which is half the period of the shear flow profile. In their theory, incompressibility is not assumed but obtained as a result of an adiabatic elimination method.

Finally, we emphasize that the periodic boundary conditions, with which the simulations were carried out, obviously play a crucial role in the formation of a shear flow profile and of the density and temperature profiles, presented in (18) and (26) respectively. Indeed, once the typical size of the vortex patterns becomes comparable to the length L of the system for $\tau > \tau_{cr} = L^2/\mathscr{D}_\perp$, the artificial periodic boundary conditions start to affect the evolution of the system. Consequently, the long time regime $\tau \gg \tau_{cr}$ described by the stationary solution is of less physical interest than the

regime of unstable growth $\tau \ll \tau_{cr}$, where the typical size of the vortex patterns remains small compared to the length L of the system. A thermodynamically large system is always in the unstable growth regime. Unfortunately, the only analytic 'large' time results for the unstable growth regime of granular fluids in *thermodynamically large* systems, have been obtained from fluctuating (linear) hydrodynamic equations or from mode coupling theory,[23, 30] but not from truly nonlinear theories. An exception is a dilute gas of inelastic point particles in one dimension,[25] where strong evidence supports the conjecture that the large space-time behavior is described by the adhesion model and the Burgers equation.

APPENDIX A: FIXED POINT SOLUTIONS AND THEIR ASYMPTOTIC STABILITY

First, we show that the fixed point solutions with non-vanishing $\mathsf{S}_{\mathbf{k}}(\infty)$ have to have the form

$$\left\{ \frac{1}{V^2} \sum_{\mathbf{k}_u} |\mathsf{S}_{\mathbf{k}_u}|^2 = \frac{d}{2} (\gamma_0 - \mathscr{D}_\perp k_u^2)/\mathscr{D}_\perp, \mathsf{S}_{\mathbf{k}} = 0 \text{ if } |\mathbf{k}| \neq k_u \right\} \tag{A.1}$$

where $\sum_{\mathbf{k}_u}$ is summation over wave numbers $\mathbf{k}_u$ that satisfy $|\mathbf{k}_u| = k_u$ with a given $k_u < k_\perp^*$. If we consider any fixed point solution that possesses a non-vanishing $\mathsf{S}_{\mathbf{k}_1}(\infty)$ and a non-vanishing $\mathsf{S}_{\mathbf{k}_2}(\infty)$ with $|\mathbf{k}_1| \neq |\mathbf{k}_2|$, we see that the relation (12) can not be fulfilled for the both cases $\mathbf{k} = \mathbf{k}_1$ and $\mathbf{k} = \mathbf{k}_2$. Therefore, this type of fixed point solutions are prohibited. Besides, from (12) a non-vanishing $\mathsf{S}_{\mathbf{k}}(\infty)$ is not allowed if $|\mathbf{k}| > k_\perp^*$. Hence, from (12) we conclude that only the type of fixed point solutions given by (A.1) is possible.

Next, we discuss asymptotic stability of these fixed point solutions. If we express a state of the order parameter $\{\mathsf{S}_{\mathbf{k}}\}$ as a vector in a vector space spanned by all independent components of $\{\mathsf{S}_{\mathbf{k}}\}$, the energy functional (11) is a function of this vector. Although a linear stability analysis of (10) is straightforward and it gives detailed information of geometry around fixed points in the vector space, we will give here only a simple argument that is enough for our purpose.

We first show that any fixed points that satisfy (A.1) with $k_u \neq k_0$ in the vector space are saddle points. Consider a fixed point solution that satisfies (A.1) with $k_u \neq k_0$ and a small perturbation $\{\delta\mathsf{S}_{\mathbf{k}} \neq 0 \text{ if } |\mathbf{k}| < k_u, \delta\mathsf{S}_{\mathbf{k}} = 0 \text{ otherwise}\}$ around it. Then the evolution equation for this small

perturbation is given by the Eq. (10) linearized around the fixed point solution, i.e.,

$$\begin{aligned}\partial_\tau\, \delta \mathbf{S}_{\mathbf{k}} &= \left\{ \gamma_0 - \mathscr{D}_\perp k^2 - \frac{2\mathscr{D}_\perp}{dV^2} \sum_{\mathbf{k}_u} |\mathbf{S}_{\mathbf{k}_u}|^2 \right\} \delta \mathbf{S}_{\mathbf{k}} \\ &= \mathscr{D}_\perp (k_u^2 - k^2)\, \delta \mathbf{S}_{\mathbf{k}} \end{aligned} \tag{A.2}$$

for $|\mathbf{k}| = k < k_u$. Because $k < k_u$, the linearized equation (A.2) implies the fixed point solutions that satisfy (A.1) with $k_u \neq k_0$ are unstable against a small perturbation in the directions of $\mathbf{S}_{\mathbf{k}}$ with $|\mathbf{k}| < k_u$ in the vector space. The similar argument for a small perturbation $\{\delta \mathbf{S}_{\mathbf{k}} \neq 0$ if $|\mathbf{k}| > k_u$, $\delta \mathbf{S}_{\mathbf{k}} = 0$ otherwise$\}$ around the fixed point shows that there exist stable directions. Therefore we conclude that these fixed points that satisfy (A.1) with $k_u \neq k_0$ are saddle points.

The energy functional (11) gives the same value for any fixed points that satisfy (A.1) with $k_u = k_0$. Because the energy functional (11) is bounded from below, a hypersphere in the vector space that is determined by (A.1) with $k_u = k_0$ forms the minimum of the energy functional that is infinitely degenerate, as symbolically illustrated in Fig. 3.

ACKNOWLEDGMENTS

M.E. acknowledges stimulating discussion with E. Ben-Naim, R. Desai and R. Kapral. J.W. and R.B. acknowledge support of the foundation "Fundamenteel Onderzoek der Materie (FOM)," which is financially supported by the Dutch National Science Foundation (NWO). J.W. also acknowledges support of a Huygens scholarship. R.B. wants to thank the Institute for Theoretical Physics of Universiteit Utrecht for its hospitality. R.B. is supported by Grant DGES-PB97-0076 (Spain).

REFERENCES

1. S. R. Nagel, *Rev. Mod. Phys.* **64**:321 (1992).
2. C. S. Campbell, *Annu. Rev. Fluid Mech.* **22**:57 (1990).
3. W. Losert, L. Bocquet, T. C. Lubensky, and J. P. Gollub, *Phys. Rev. Lett.* **85**:1428 (2000). L. Bocquet, W. Losert, D. Schalk, T. C. Lubensky, and J. P. Gollub, *Phys. Rev. E* **65**:U11307 (2001).
4. P. B. Umbanhowar, F. Melo, and H. L. Swinney, *Nature* **382**:793 (1996).
5. G. P. Collins, *Sci. Am.* **284** (1):17 (2001).
6. E. R. Nowak, J. B. Knight, E. Ben-Naim, H. M. Jaeger, and S. R. *Nagel, Phys. Rev. E* **57**:1971 (1998). J. S. Olafsen and J. S. Urbach, *Phys. Rev. Lett.* **81**:4369 (1998).
7. D. R. Williams and F. C. MacKintosh, *Phys. Rev. E* **54**:R9 (1996). G. Peng and T. Ohta, *Phys. Rev. E* **58**:4737 (1998). C. Bizon, M. D. Shattuck, J. B. Swift, and H. L. Swinney,

Phys. Rev. E **60**:4340 (1999). A. Puglisi, V. Loreto, U. Marini Bettolo Marconi, A. Petri, and A. Vulpiani, *Phys. Rev. Lett.* **81**:3848 (1998). A. Puglisi, V. Loreto, U. Marini Bettolo Marconi, and A. Vulpiani, *Phys. Rev. E* **59**:5582 (1999). T. P. C. van Noije, M. H. Ernst, E. Trizac, and I. Pagonabarraga, *Phys. Rev. E* **59**:4326 (1999).

8. J. T. Jenkins and M. W. Richman, *Phys. Fluids* **28**:3485 (1985). J. T. Jenkins and S. B. Savage, *J. Fluid Mech.* **130**:187 (1983).
9. I. Goldhirsch and G. Zanetti, *Phys. Rev. Lett.* **70**:1619 (1993). I. Goldhirsch, M-L. Tan, and G. Zanetti, *J. Scient. Comp.* **8**:1 (1993).
10. R. Soto, M. Mareschal, and M. Malek Mansour, *Phys. Rev. E* **62**:3836 (2000).
11. P. C. Hohenberg and B. I. Halperin, *Rev. Mod. Phys.* **49**:435 (1977).
12. L. Landau and E. M. Lifshitz, *Fluid Mechanics* (Pergamon Press, 1959).
13. J. J. Brey, J. W. Dufty, and A. Santos, *J. Stat. Phys.* **87**:1051 (1997).
14. J. A. G. Orza, R. Brito, T. P. C. van Noije, and M. H. Ernst, *Int. J. Mod. Phys. C* **8**:953 (1997).
15. T. P. C. van Noije, M. H. Ernst, R. Brito, and J. A. G. Orza, *Phys. Rev. Lett.* **79**:411 (1997).
16. T. P. C. van Noije, M. H. Ernst, and R. Brito, *Phys. Rev. E* **57**:R4891 (1998).
17. P. K. Haff, *J. Fluid Mech.* **134**:401 (1983).
18. S. McNamara, *Phys. Fluids A* **5**:3056 (1993).
19. P. Deltour and J.-L. Barrat, *J. Phys. I France* **7**:137 (1997).
20. J. J. Brey, F. Moreno, and J. W. Dufty, *Phys. Rev. E* **54**:445 (1996)
21. S. E. Esipov and T. Pöschel, *J. Stat. Phys.* **86**:1385 (1997).
22. T. P. C. van Noije and M. H. Ernst, *Phys. Rev. E* **61**:1765 (2000).
23. R. Brito and M. H. Ernst, *Europhys. Lett.* **43**:497 (1998). R. Brito and M. H. Ernst, *Int. J. Mod. Phys. C* **9**:1339 (1998).
24. J. J. Brey, M. J. Ruiz-Montero, and D. Cubero, *Phys. Rev. E* **60**:3150 (1999).
25. E. Ben-Naim, S. Y. Chen, G. D. Doolen, and S. Redner, *Phys. Rev. Lett.* **83**:4069 (1999).
26. J. Wakou, to be published.
27. G. K. Batchelor, *The Theory of Homogeneous Turbulence* (Cambridge University Press, 1970).
28. U. Frisch, *Turbulence: The legacy of A. N. Kolmogorov* (Cambridge University Press, 1996).
29. E. Trizac and A. Barrat, *Eur. Phys. J. E.* **3**:291 (2000).
30. S. Chen, Y. Deng, X. Nie, and Y. Tu, *Phys. Lett. A* **269**:218 (2000).